Supplementary Information

Photophoretic assembly and migration of dielectric particles and Escherichia coli in liquids using a subwavelength diameter optical fiber

Hongxiang Lei‡, Yao Zhang‡, Xingmin Li, and Baojun Li*

State Key Laboratory of Optoelectronic Materials and Technologies, School of Physics and Engineering, Sun Yat-Sen University, Guangzhou 510275, China.

‡These authors contributed equally to this work

*Email: stslbj@mail.sysu.edu.cn

1. Assembly and diffusion of the SiO_2 particles in liquids

After the laser is on with a power of 200 mW, the suspended SiO_2 particles (3.14-μm diameter) moved toward the SDF (910-nm diameter, 205-μm length). The assembled particles keep increasing during the laser-on duration t_{on}. The number N of the assembled particles reach about 640, 1450, 2000, 2580, 3400 and 4180 at t_{on} = 40 s (Fig. S1a), t_{on} = 90 s (Fig. S1b), t_{on} = 140 s (Fig. S1c), t_{on} = 200 s (Fig. S1d), t_{on} = 270 s (Fig. S1e) and t_{on} = 340 s (Fig. S1f), respectively. Once the laser is off, the leaking light from the SDF vanishes and the SiO_2 particles are no longer non-uniformly heated, leading to the evanishment of the photophoretic forces. Accordingly, the particles stop their photophoretic motions and begin to diffuse back to a dispersed state via Brownian motions. At the moment of the laser off, the photophoretic motions of the SiO_2 particles stop immediately but still assemble around the SDF. In this case, the area occupied by the assembled particles is about 38,800 μm^2 (Fig. S2a). Then they are gradually dispersed away with an increase of laser-off time. Accordingly, the calculated area occupied by the assembled particles are about 40,600, 43,000, 45,000, 46,800, and 48,200 μm^2 after t_{off} = 10 s (Fig. S2b), t_{off} = 50 s (Fig. S2c), t_{off} = 100 s (Fig. S2d), t_{off} = 150 s (Fig. S2e), and t_{off} = 200 s (Fig. S2f), respectively.

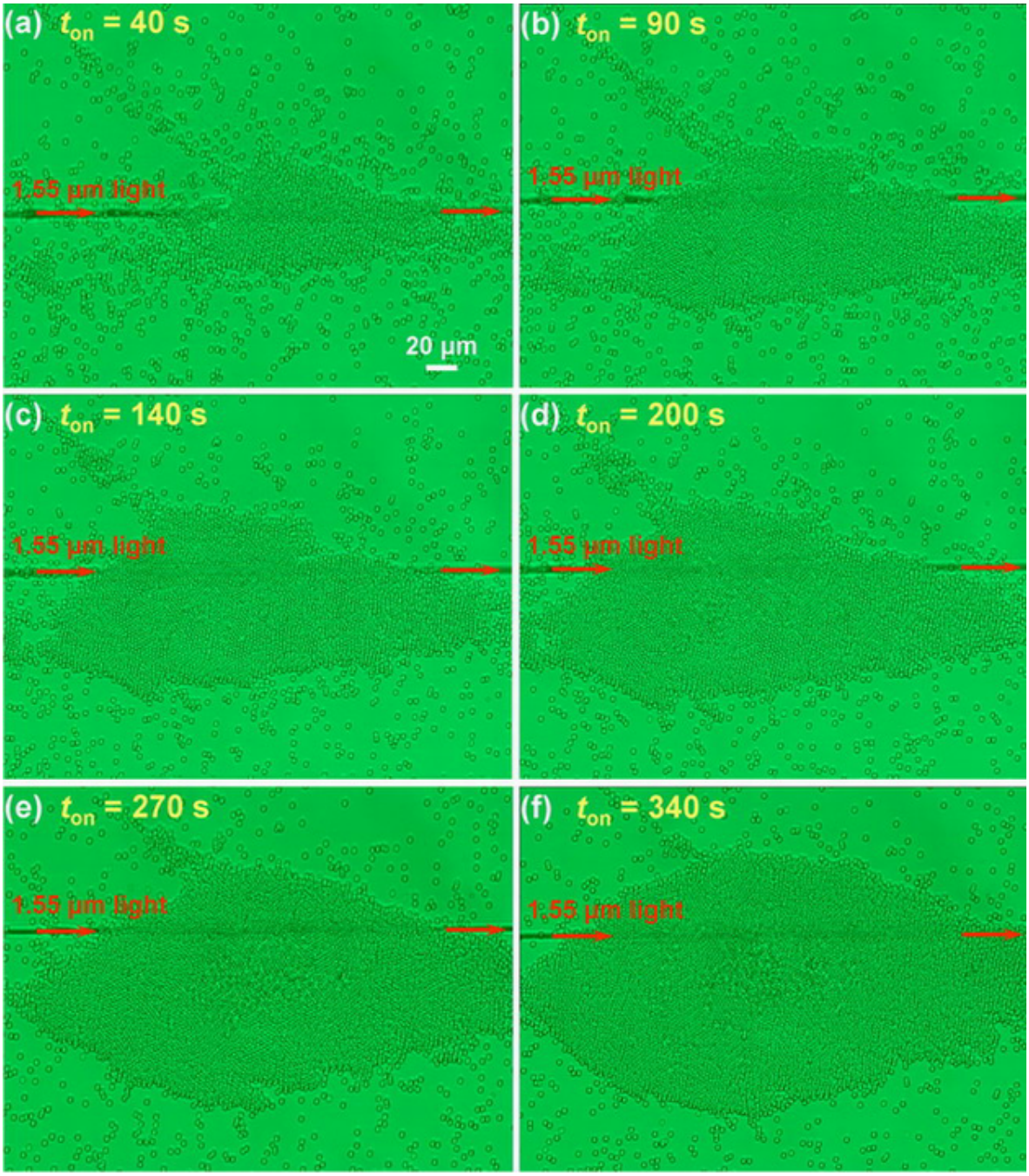

FIG. S1. CCD captured microscope images of the SiO_2 particles assembled from t_{on} = 40 to 340 s. (a) t_{on} = 40 s. (b) t_{on} = 90 s. (c) t_{on} = 140 s. (d) t_{on} = 200 s. (e) t_{on} = 270 s. (f) t_{on} = 340 s.

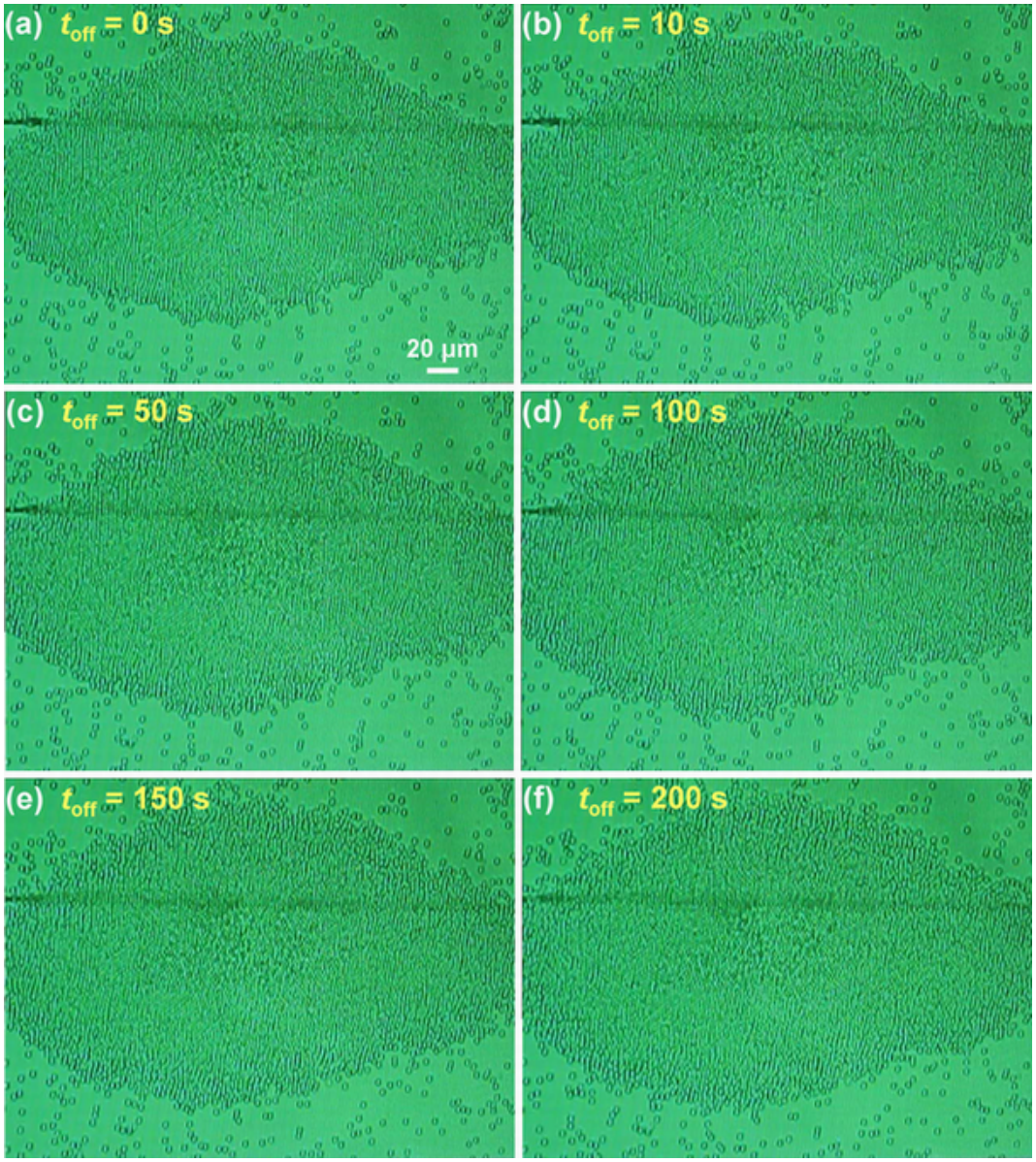

FIG. S2. CCD captured microscope images of the SiO_2 particles diffused from t_{off} = 0 to 200 s. (a) t_{off} = 0 s. (b) t_{off} = 10 s. (c) t_{off} = 50 s. (d) t_{off} = 100 s. (e) t_{off} = 150 s. (f) t_{off} = 200 s.

2. Assembly and diffusion of the Escherichia coli in liquids

The assembly and diffusion of the Escherichia coli around a SDF (1.2-μm diameter, 200-μm length) are similar with those of the SiO_2 particles. The number N of the assembled Escherichia coli are about 495, 600, 685, 760, 820 and 870 at t_{on} = 20 s (Fig. S3a), t_{on} = 25 s

(Fig. S3b), t_{on} = 30 s (Fig. S3c), t_{on} = 35 s (Fig. S3d), t_{on} = 40 s (Fig. S3e) and t_{on} = 45 s (Fig. S3f), respectively. Once the laser is off, the Escherichia coli stop their photophoretic motions but still assemble around the SDF. In this case, the area occupied by assembled Escherichia coli is about 3,500 μm^2 (Fig. S4a). Then they are gradually dispersed away with an increase of laser-off time. Accordingly, the calculated areas occupied by the assembled Escherichia coli are 3,900, 4,500, 5,200, 6,000 and 7,000 μm^2 after t_{off} = 5 s (Fig. S4b), t_{off} = 25 s (Fig. S4c), t_{off} = 45 s (Fig. S4d), t_{off} = 65 s (Fig. S4e) and t_{off} = 85 s (Fig. S4f), respectively. It should be noticed that the diffusion of the Escherichia coli is a bit faster than that of the SiO_2 particles. This is because the living Escherichia coli also diffuse via their own swarming beside Brownian motions.

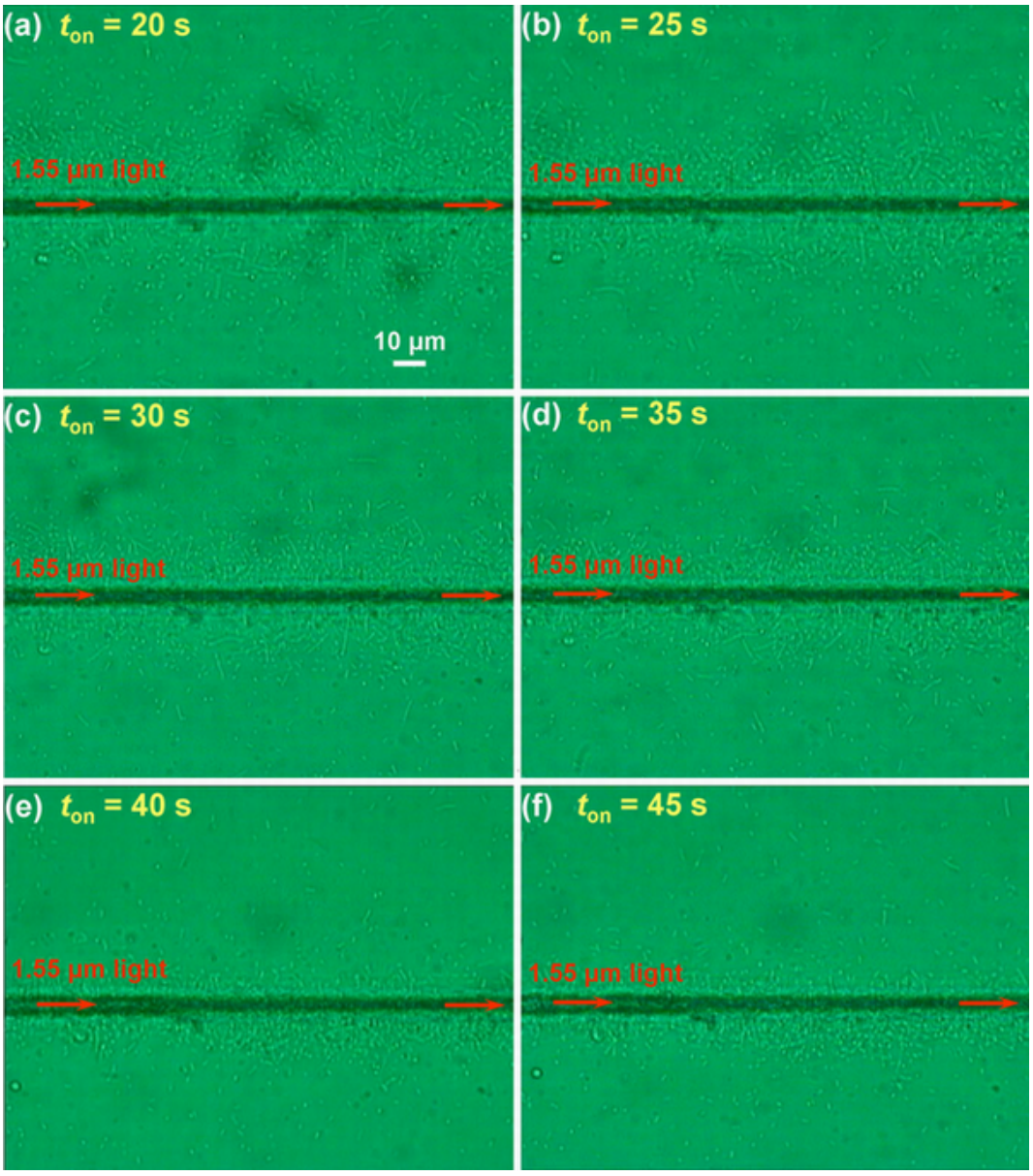

FIG. S3. CCD captured microscope images of the Escherichia coli assembled from t_{on} = 20 to 45 s. (a) t_{on} = 20 s. (b) t_{on} = 25 s. (c) t_{on} = 30 s. (d) t_{on} = 35 s. (e) t_{on} = 40 s. (f) t_{on} = 45 s.

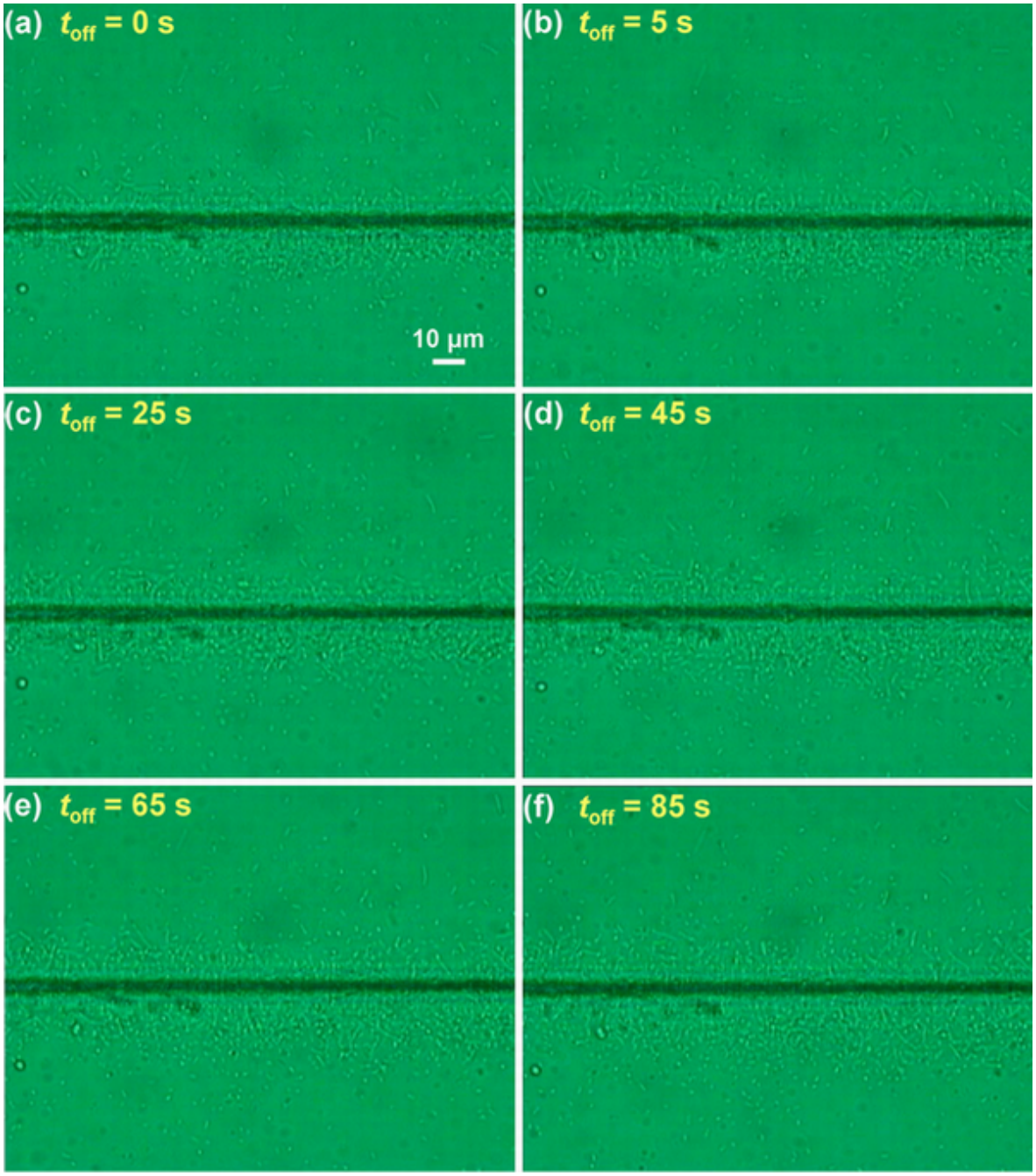

FIG. S4. CCD captured microscope images of the Escherichia coli diffused from t_{off} = 0 to 85 s. (a) t_{off} = 0 s. (b) t_{off} = 5 s. (c) t_{off} = 25 s. (d) t_{off} = 45 s. (e) t_{off} = 65 s. (f) t_{off} = 85 s.

3. Assembly of red blood cells in blood and cell culture media

To show the capability of this method on cells in biologic media like blood and cell culture media, the assembly of red blood cells (RBCs) of pigeon in blood and RBCs of chicken in cell culture media was performed. Figures S5a and b show the assembly process of the pigeon RBCs in blood using a 900-nm-diameter SDF. It can be seen that, without optical power (i.e. t_{on} = 0 s, t_{on} denotes laser-on duration), the RBCs were randomly dispersed in the diluted blood (Fig. S5a). Once the laser was on with an optical power of 100 mW, the RBCs started to move toward the SDF. At t_{on} = 660 s, about 150 RBCs were assembled around the SDF (Fig. S5b). It should be pointed out that, due to high concentration of the RBCs in original blood, to clear show the assembly process, the high concentration RBCs were diluted with deionized water (volume ratio of RBCs to water ~1:800). Figures S5c and d show the assembly of the chicken RBCs in cell culture media using a 950-nm-diameter SDF. It can be seen that, without optical power (i.e. t_{on} = 0 s), the RBCs were randomly dispersed in the cell culture media (Fig. S5c). Once the laser was on with an optical power of 200 mW, the RBCs started to move toward the SDF. At t_{on} = 660 s, about 40 RBCs were assembled around the SDF (Fig. S5d). These experiments indicate that the assembly of RBCs in cell culture media is weaker than those of RBCs in diluted blood and dielectric particles/Escherichia coli in water. This is because the NaCl solute of the cell culture media has a larger refractive index (n = 1.531) than that of water and thus the average index of the cell culture media is larger than that of water, which will weaken the photophoretic force exerted on the suspended objects.

4. Selective assembly of particles in different sizes from mixture

Particles with a low absorption coefficient at the incident wavelength can be assembled by the negative photophoretic force. The photophoretic velocity depends on the diameter and the refractive index of the particles. According to our calculations and analyses, particles with larger diameter or higher index will lead to larger photophoretic velocity. Therefore, if the photophoretic velocity of one kind of particles (with a larger diameter or a higher index) is significantly larger than that of the other one, it is possible

to selectively assemble the particles from a mixture. We have performed the selective assembly of larger particles from a mixture of suspended SiO_2 particles with diameter of 2.08 and 5.65 μm through a 1.45-μm-diameter SDF. Figure S6 shows the selective assembly of the 5.65-μm-diameter SiO_2 particles by using the SDF with an incident optical power of 200 mW at 1.55 μm. Actually, the particles in both diameters were assembled. However, due to the considerable difference in the average photophoretic velocity, the 5.65-μm diameter particles were assembled in the inner region (closer to the SDF) while the 2.08-μm diameter particles were assembled in the outer region. According to our experimental results, the limitation of the selective assembly occurred in a mixture is that the diameter or index of the target particles is over twice larger than that of the other particles.

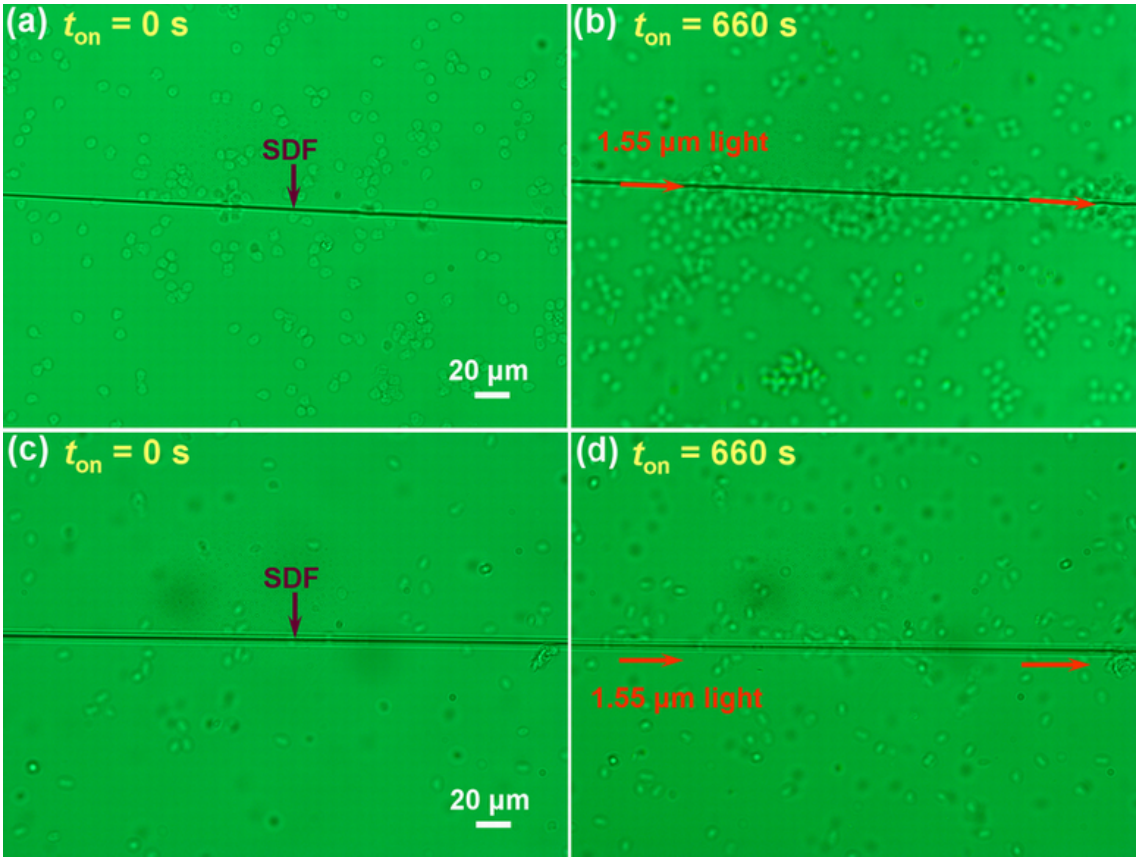

FIG. S5. Assembly of pigeon RBCs in diluted blood and chicken RBCs in culture media. (a–b) CCD captured microscope images for assembly of the pigeon RBCs in diluted blood using a 900-nm-diameter SDF without incident optical power (a, t_{on} = 0 s) and with an incident optical power of 200 mW (b, t_{on} = 660 s). (c–d) CCD captured microscope images for assembly of the chicken RBCs in cell culture media using a

950-nm-diameter SDF without incident optical power (c, t_{on} = 0 s) and with an incident optical power of 100 mW (d, t_{on} = 660 s).

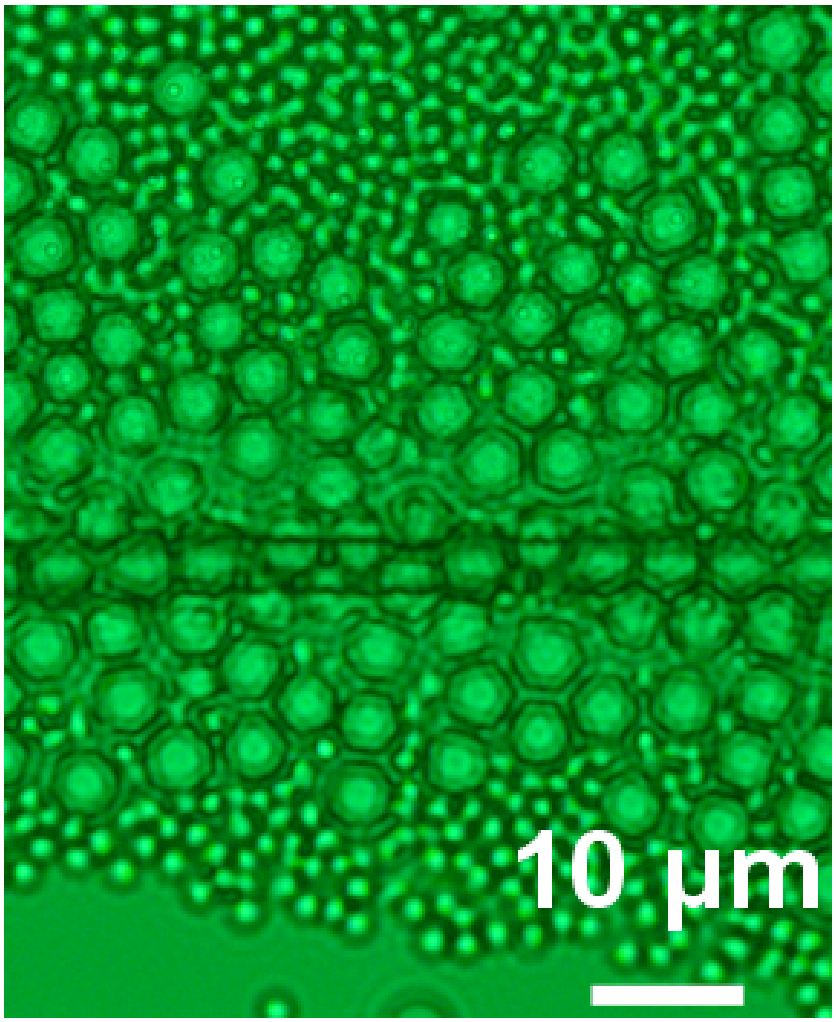

FIG. S6. Selective assembly of SiO_2 particles with diameters of 2.08 and 5.65 μm from a mixture.

5. Electric field amplitude at the surfaces of SDFs with different diameters

The normalized electric field amplitude *E* at the surface of SDFs with different diameters was obtained by the 3D FDTD simulations at the wavelength of 1.55 μm, as shown in Fig. S7. It can be seen that the value of *E* reaches a maximum of 0.92 at the surface of a SDF with a diameter of 1.3 μm. This means, at the incident wavelength of

1.55 μm, the SDF with a diameter of 1.3 μm provides the largest photophoretic force on the particles, which can be considered as an optimized setup for particle assembly.

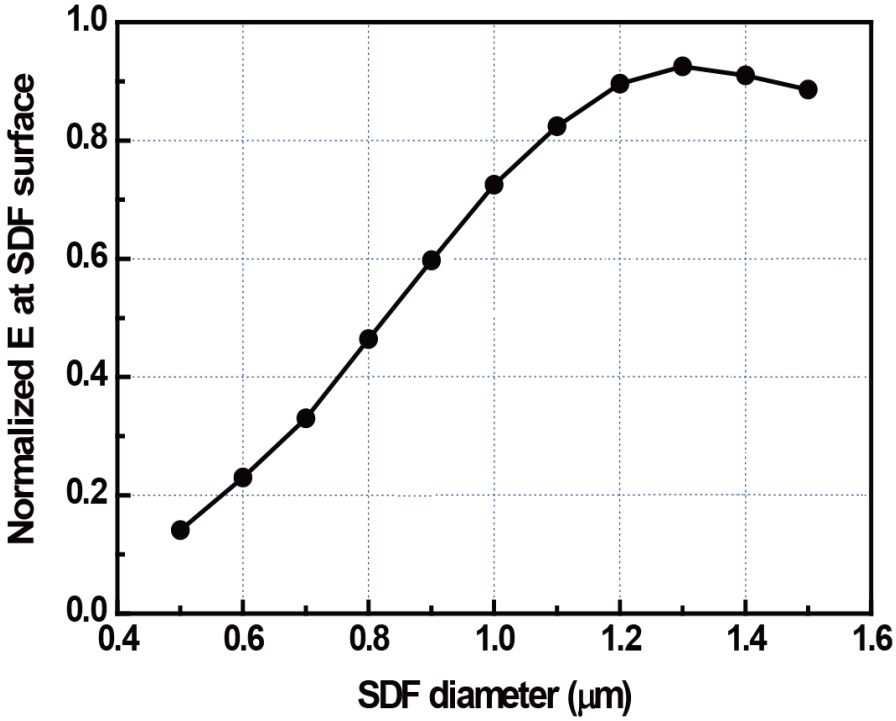

FIG. S7. Normalized electric field amplitude at the SDF surface with different diameters at the wavelength of 1.55-μm.

6. Assembly of SiO2 particles in fluidic channel

To demonstrate the applicability of this method in a fluidic channel, a SDF (1.4 μm in diameter and 330 μm in length) (Fig. S8a) was placed in the channel which was formed by etching a quartz plate with hydrofluoric acid. The width and depth of the channel are 715 and 105 μm, respectively (Fig. S8b). For example, when a 1.55-μm light with an optical power of 200 mW was launched into the SDF for 220 s, about 300 particles were assembled around the SDF (Fig. S8c).

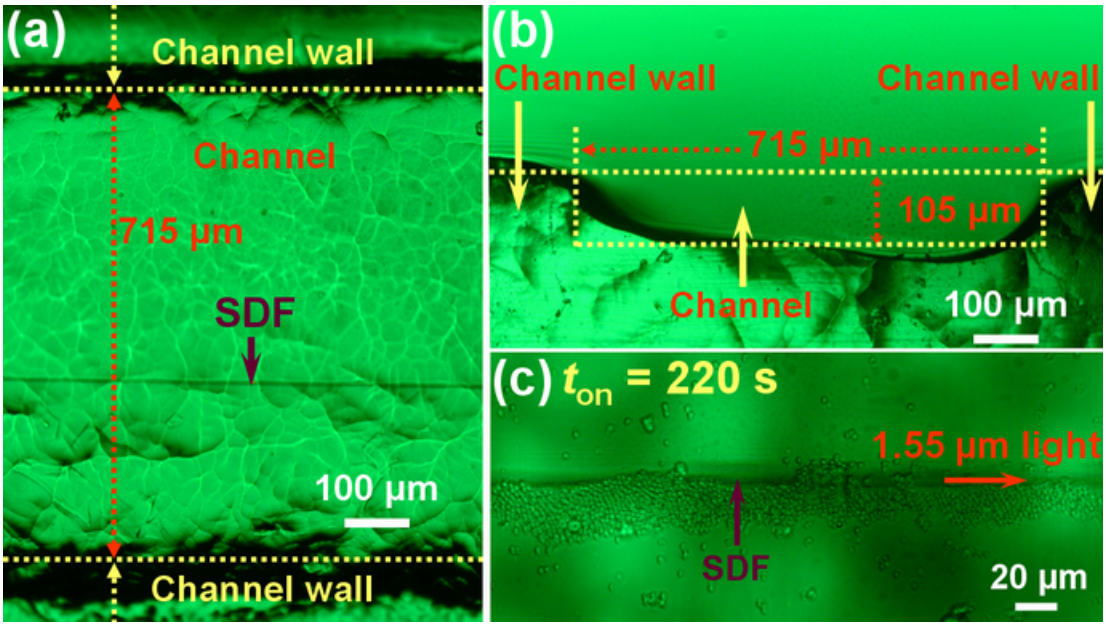

FIG. S8. Assembly of SiO_2 particles in a fluidic channel. (a) Microscope image of the SDF placed in the fluidic channel. (b) Microscope image of the cross section of the fluidic channel. (c) After launching an optical power of 200 mW into the SDF for 220 s, about 300 particles were assembled.

7. Impact of flowing surrounding on the assembly of particles

We have also investigated the impact of a flowing surrounding on the particle assembly. After launching an optical power of 200 mW into a 1.4-μm-diameter SDF in stationary droplet for 220 s, about 300 SiO_2 particles (3.14-μm diameter) were assembled around the SDF. Then a water flow with different flow rates at a direction perpendicular to the SDF was introduced by using a syringe pump. As an example, the case for the flow rate of 4 μm/s is included in the Supplementary Information (Fig. S9). The results indicate that the assembly process occurs but the assembly region shifted to about 60 μm below the SDF, i.e., to the downstream due to the dragging force of the flow. With the increase of the time duration of the flow applied (denoted by t_f), the number of the particles assembled in the re-assembly region keeps increasing. The number of the re-assembled particles reach about 80, 200, 350, and 500 at t_f = 50 s (Fig. S9a), t_f = 150 s (Fig. S9b), t_f = 250 s (Fig. S9c), and t_f = 350 s (Fig. S9d), respectively. The results indicate that despite of the shift of the assembly region, the particles can still be assembled in a flowing fluidic

surrounding. According to our experiments for different flow rates, the limitation of flow rate to the assembly is the peak of the photophoretic velocity (at a certain laser-on duration). This is because in this case, the photophoretic force on the particles will be totally counteracted by the dragging force of the flow. Moreover, the assembly of particles with larger diameter or higher index can bear the impact of water flow with a larger flow rate, which is attributed to the stronger photophoretic forces exerted on these particles.

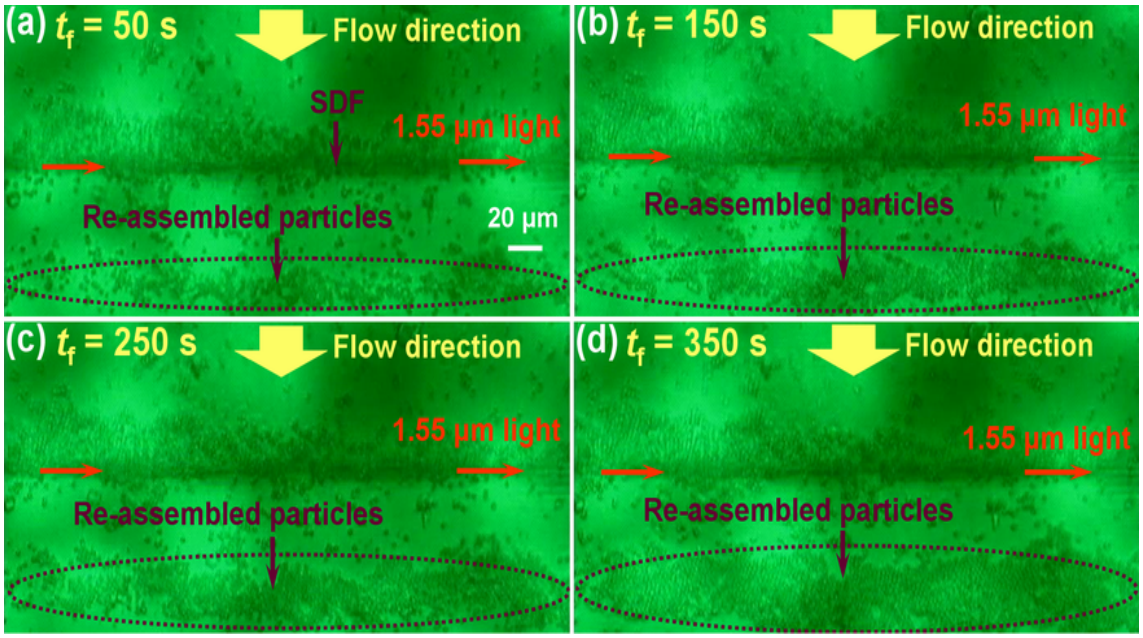

FIG. S9. The impact of flowing surrounding on the assembly of 3.14-μm-diameter SiO_2 particles by using a 1.4-μm-diameter SDF. The yellow arrows show the follow direction which perpendicular to the SDF while the red arrows show the propagation direction of the 1.55 μm light in the SDS. The flow rate is 4μm/s. t_f denotes the time duration of the flow applied.

8. Photophoretic velocity analysis of the particles in liquids

According to the theoretical study presented by Soong *et al*,[1] photophoretic velocity V_{ph} of particles in liquids can be expressed as

$$V_{ph} = -\frac{\beta_T A r_0^2}{18\mu v_0 k_f} I J_1 \frac{\ln 3 + 4(\ln 3 - 1)L_s / r_0}{(k_p / k_f + 2)(1 + 2L_s / R)} \quad (1)$$

Where:

β_T: the cubic thermal expansion coefficient of the solvent (water)

A: the Hamaker constant

r_0: the radius of solvent (water) molecule

μ: the fluid viscosity

v_0: the specific molecular volume of water

k_f: the thermal conductivity of water

I: the intensity of the incident light the particle subjected

J_1: the energy distribution asymmetry factor

k_p: the thermal conductivity of the particle

L_s: the slip length (particles relative to fluid)

R: the radius of the particles

According to Eq. (1), it is known that as long as the particles and the solvent are determined, V_{ph} is only governed by I and J_1 because the other parameters become constants. For the cases in our experiments, I and J_1 are both related to the distance d from the particles to the SDF. This is confirmed by the experimental results of V_{ph}.

The value of J_1 is mainly determined by the electromagnetic field distributions near the particle, and governed by the field profiles of the leaking light. Actually, the value of J_1 becomes larger when the cross-section of the field profile of the leaking light is close to the one of a plane wave, and becomes smaller when it closes to the one of a spherical wave. As d increases, the field profiles of the leaking light which radiates the particles become close to the one of the plane wave. Therefore, the value of J_1 gradually increases as d increases. Due to the decay of the leaking light, the value of I gradually decreases as d increases. With the increasing d, the value of J_1 increases faster at first and then slower than I decreases. As a result, the product IJ_1 exhibits a tendency that it ascends at first and then descends with an increasing d, leading to a peak value at a certain d. With the laser-on duration t increases, the assembled particles increase and surround the SDF to gradually reduce the extension of leaking lights. In this case, the field profiles of the leaking light around the SDF gradually minish proportionally, leading to the position of the peak V_{ph} moves toward the SDF. These are also confirmed by the experimental results of V_{ph}.

Reference

1. C. Y. Soong, W. K. Li, C. H. Liu, and P. Y. Tzeng, Opt. Express **18**, 2168 (2010).